Life Sciences 227 (2019) 201–211

Contents lists available at ScienceDirect

Life Sciences

journal homepage: www.elsevier.com/locate/lifescie

Abnormality of hepatic triglyceride metabolism in $Apc^{Min/+}$ mice with colon cancer cachexia

Biao Yu[1], Mingjun Zhang[1], Jiahuan Chen, Lingyu Wang, Xiaohuan Peng, Xinwei Zhang, He Wang, Anbei Wang, Dazhong Zhao, Daxin Pang, Hongsheng OuYang, Xiaochun Tang*

Jilin Provincial Key Laboratory of Animal Embryo Engineering, College of Animal Sciences, Jilin University, No.5333 Xi'an Road, Lvyuan District, Changchun 130062, Jilin Province, China

ARTICLE INFO

Keywords:
Adenomatous polyposis coli
GPIHBP1
Hypertriglyceridemia
Oct-1
NF-κB
Colorectal cancer

ABSTRACT

Aims: Colorectal cancer syndrome has been one of the greatest concerns in the world. Although several epidemiological studies have shown that hepatic low lipoprotein lipase (LPL) mRNA expression may be associated with dyslipidemia and tumor progression, it is still not known whether the liver plays an essential role in hyperlipidemia of $Apc^{Min/+}$ mice.

Main methods: We measured the expression of metabolic enzymes that involved fatty acid uptake, de novo lipogenesis (DNL), β-oxidation and investigated hepatic triglyceride production in the liver of wild-type and $Apc^{Min/+}$ mice.

Key findings: We found that hepatic fatty acid uptake and DNL decreased, but there was no significant difference in fatty acid β-oxidation. Interestingly, the production of hepatic very low-density lipoprotein-triglyceride (VLDL-TG) decreased at 20 weeks of age, but marked steatosis was observed in the livers of the $Apc^{Min/+}$ mouse. To further explore hypertriglyceridemia, we assessed the function of hepatic glycosylphosphatidylinositol-anchored high-density lipoprotein binding protein 1 (GPIHBP1) for the first time. GPIHBP1 is governed by the transcription factor octamer-binding transcription factor-1 (Oct-1) which are involved in the nuclear factor-κB (NF-κB) signaling pathway in the liver of $Apc^{Min/+}$ mice. Importantly, it was also confirmed that sn50 (100 μg/mL, an inhibitor of the NF-κB) reversed the tumor necrosis factor α (TNFα)-induced Oct-1 and GPIHBP1 reduction in HepG2 cells.

Significance: Altogether, these findings highlighted a novel role of GPIHBP1 that might be responsible for hypertriglyceridemia in $Apc^{Min/+}$ mice. Hypertriglyceridemia in these mice may be associated with their hepatic lipid metabolism development.

1. Introduction

Cachexia is a metabolic syndrome characterized by severe losing of muscle mass and adipose tissue, is a common complication of end-stage cancers, especially colorectal cancer [1]. It is therefore important to study the effect of cachexia progression not only on body weight but also on underlying ailment events such as chronic inflammation, insulin resistance, increased gut permeability, dyslipidemia, anorexia, splenomegaly and disrupted metabolism [2].

$Apc^{Min/+}$ mouse is an animal model for human familial adenomatous polyposis (FAP). It has been reported that an age-dependent hyperlipidemia state is associated with the loss of body weight and impaired adipogenesis in $Apc^{Min/+}$ mice [3,4]. Mutation of normal adenomatous polyposis coli (APC) function induces intestinal polyp development with activating of the Wnt/β-catenin signaling pathways [5,6]. In addition, severely cachectic $Apc^{Min/+}$ mice have elevated levels of serum endotoxin and increased gut permeability that is accompanied by inflammation and hyperlipidemia, which can also affect the liver [7].

In the present study, the downregulated expression of free fatty acids uses genes in the white adipose tissue (WAT) of $Apc^{Min/+}$ mice is much lower than that of WT mice. The changed gene expression may lead to the inability of serum lipid being catabolized and stored at WAT, which in turn leads to reduced adipogenesis, but elevated serum lipid level [8]. Moreover, It is commonly associated with the increase of acute phase proteins and pro-inflammatory cytokines in plasma,

* Corresponding author.
E-mail address: xiaochuntang@jlu.edu.cn (X. Tang).
[1] These authors contributed equally to the work.

https://doi.org/10.1016/j.lfs.2019.04.041
Received 2 January 2019; Received in revised form 10 April 2019; Accepted 16 April 2019
Available online 17 April 2019

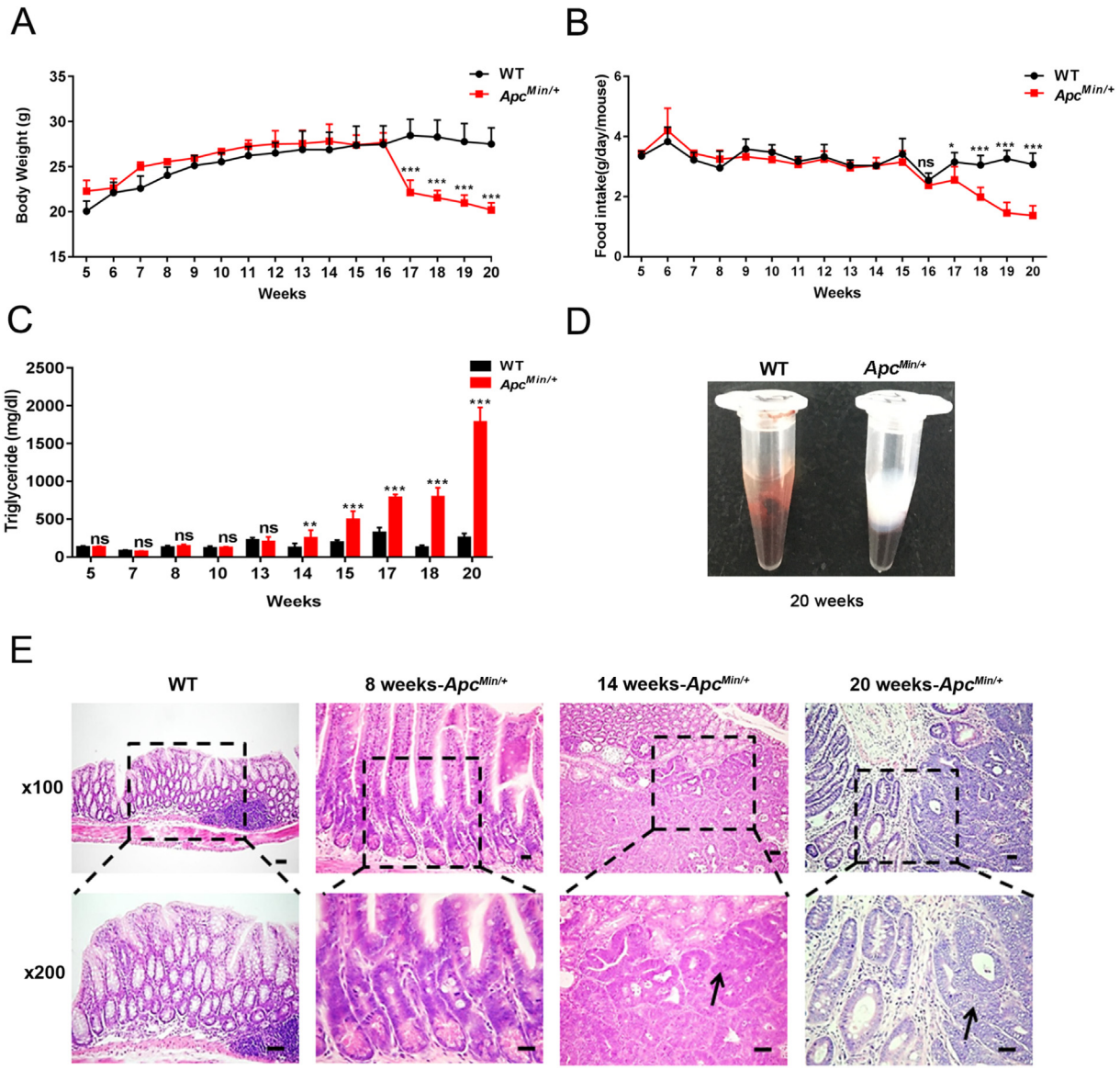

Fig. 1. Age-dependent increase of serum lipid level in $Apc^{Min/+}$ mice. 4–5 weeks old $Apc^{Min/+}$ (Min, $n = 20$) and wild-type (WT, $n = 20$) mice were housed in plastic cages (≤ 5 mice per cage). (A and B) Food intake and body weight were monitored from the point at which the diet was initiated until the end of the experiment ($n \geq 5$). (C) After fasting, serum TGs were measured from 5 to 20 weeks in $Apc^{Min/+}$ mice ($n \geq 5$). (D) Lactescent serum of the $Apc^{Min/+}$ mouse (right picture) and the normal serum of WT mouse (left picture) at 20 weeks ($n \geq 5$). (E) H&E stain showing cachexia (black arrow) in the intestine at 14 and 20 weeks of age in $Apc^{Min/+}$ mice ($n = 3$, respectively). Magnification, ×100 and ×200, Scale bars: 50 μm. Error bars represent the standard deviation. $^{**}p < 0.01$; $^{***}p < 0.001$; ns, not significant.

notably IL-6 and MCP-1 in the progression of cachexia. IL-6 and MCP-1 related to the increased tumor burden may have an important role in the intense inflammatory response during cachexia [9]. Cachexia is inhibited in an IL-6 knockout (IL-$6^{-/-}$-$Apc^{Min/+}$) mouse. Interestingly, the cachectic response can be restored by systemic IL-6 over-expression in the IL-$6^{-/-}$-$Apc^{Min/+}$ mouse, while IL-6 over-expression in C57BL/6 mice does not induce cachexia. Therefore, It is necessary but not sufficient for IL-6 to induce cachexia in mice [10]. Furthermore, increase of intestinal adenomas and hyperlipidemia were detected in C57BL/KsJ-db/db-$Apc^{Min/+}$ (db/db-Min/+) mouse, an animal model of obesity and colorectal cancer, compared to db/m-Min/+ and m/m-Min/+ mouse. It is indicated that obesity is also a risk factor of $Apc^{Min/+}$ mice intestinal adenocarcinomas development [11].

Epidemiological studies indicated that serum levels of triglycerides (TGs) and total cholesterol (TC) have presented a positive risk of colon cancer with hyperlipidemia [12–14]. As Naoko Niho notes [3], the low level of hepatic lipoprotein lipase (LPL) mRNA expression may be associated with hyperlipidemia and involved in the progression of adenoma developing to carcinoma, but the function of hepatic lipid metabolism in $Apc^{Min/+}$ mice of hyperlipidemia is not well known. Since liver governs systemic energy demands by regulating metabolic pathways, which involve hepatic uptake of plasma non-esterified free fatty acid (NFFA), de novo lipogenesis (DNL), fatty acid β-oxidation and secretion in low-density lipoprotein-triglyceride (VLDL-TG) [15,16]. It is likely that the liver is a pathological target of cachexia progression in $Apc^{Min/+}$ mice.

DNL is a metabolic pathway catalyzed by several rate-limiting enzymes and transcription factors including acetyl-CoA carboxylase 1 (ACC1), fatty acid synthase (FAS), ATP Citrate Lyase (ACLY) and sterol regulatory element binding protein (SREBP-1c), which participate in hepatic lipid metabolism [17,18]. DNL up-regulation is able to induce fatty accumulation through an increase in fatty acid synthesis. In fact, ACC1 was confirmed which is a rate-limiting enzyme of hepatic DNL [19,20]. In addition, carnitine palmitoyl transferase 1 (CPT1) is

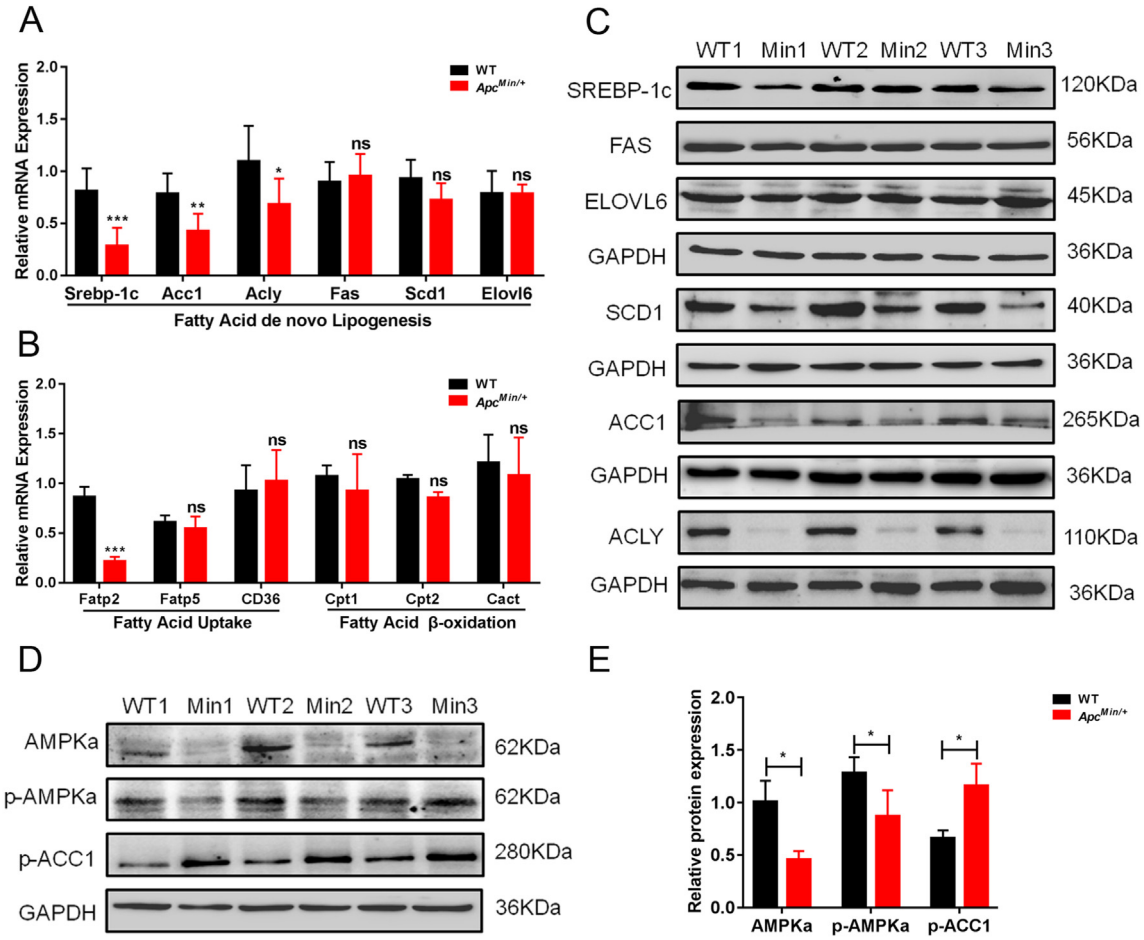

Fig. 2. Change of metabolic enzyme expression in the liver of *Apc*$^{Min/+}$ mice. (A and B) *Srebp-1c*, *Acc1*, *Acly*, *Fas*, *Scd1*, *Elovl6*, *Fatp2*, *Fatp5*, *CD36*, *Cact*, *Cpt1*, and *Cpt2* were measured by qRT-PCR in the liver of *Apc*$^{Min/+}$ and WT mouse ($n = 3$). (C) ACC1, ACLY, FAS, SCD1, ELOVL6 and SREBP-1c proteins were measured by Western Blot with specific antibodies in the liver of *Apc*$^{Min/+}$ and WT mice ($n = 3$). (D and E) AMPK pathway related proteins expression were determined using Western Blot. The densities of AMPK, p-AMPK, and p-ACC1 bounds were measured and their ratio was calculated (WT: wild-type mice, Min: *Apc*$^{Min/+}$ mice). Error bars represent the standard deviation. $^{*}p < 0.05$, $^{**}p < 0.01$ and $^{***}p < 0.001$.

responsible for mitochondria fatty acid β-oxidation [21]. VLDL-TG is a triglyceride-rich lipoprotein (TRL), which contains a hydrophobic core mainly composed of TG and TC. The secretion of hepatic VLDL-TG particles was transmitted to peripheral tissues for energy expenditure and/or storage [22]. It is reported that LPL is the main of plasma lipid metabolism in the TRLs catabolism processes, which disintegrates VLDL to higher-density and smaller-sized particles, including low-density lipoproteins (LDL) and intermediate density lipoproteins (IDL) [23].

Recently, glycosylphosphatidylinositol-anchored high-density lipoprotein binding protein 1 (GPIHBP1) was identified to have a critical role in lipolysis; GPIHBP1 was found to be responsible for the transportation of LPL into capillaries, which is involved in TGs metabolism [24,25]. Previous research illustrated LPL mislocalization with GPIHBP1 defect and LPL or GPIHBP1 mutations resulted in increased TG accumulation [26]. Additionally, GPIHBP1 plays a crucial role in the lipolytic process of the ApoB100 and ApoB48 lipoproteins in the *GPIHBP1*$^{-/-}$ mice [27,28]. Therefore, we hypothesized that GPIHBP1 may be one key factor contributing to hypertriglyceridemia in *Apc*$^{Min/+}$ mice.

The purpose of this study is to investigate if hepatic lipid metabolism affects the progression of hyperlipidemia in *Apc*$^{Min/+}$ mice. We examined whether heterozygous mutations in the mice *APC* gene lead to dramatic changes in serum TG and NFFA level. Moreover, we investigated the expression of mRNAs encoding metabolic enzymes that involved fatty acid uptake, DNL, and β-oxidation in the liver of *Apc*$^{Min/+}$ mice. Furthermore, we also performed GPIHBP1 gene expression analysis and identified several relative mechanism changes in the gene. On the basis of these data, possible regulation of hypertriglyceridemia in intestinal polyp formation is proposed in *Apc*$^{Min/+}$ mice.

2. Materials and methods

2.1. Animals

Wild-type male C57BL/6J (WT, $n = 20$) and mutant male C57BL/6J-*Apc*$^{Min/+}$ (*Apc*$^{Min/+}$, Min, $n = 20$), 4–5 week-old mice were purchased from the Nanjing Biomedical Research Institute of Nanjing University (Nanjing, China). The mice were housed in an air-conditioned room maintained at 22 ± 2 °C and 40%–60% humidity with a 12-h dark-light cycle. The mice were provided with water and food ad libitum and housed in plastic cages (5 mice per cage) in a specific pathogen-free animal facility. All animal welfare and experimental procedures were performed strictly according to the guidelines from the National Institutes of Health Guide for the Care and Use of Laboratory Animals (NIH Publications No. 8023, revised 1978). Additionally, the procedures were approved by the Institutional Animal Care and Use Committee of Jilin University under the approved protocol number 201707025.

2.2. Hepatic Triglyceride Production Tests (HTPTs)

As previously reported [7], the mice were sacrificed at 7–8 weeks of

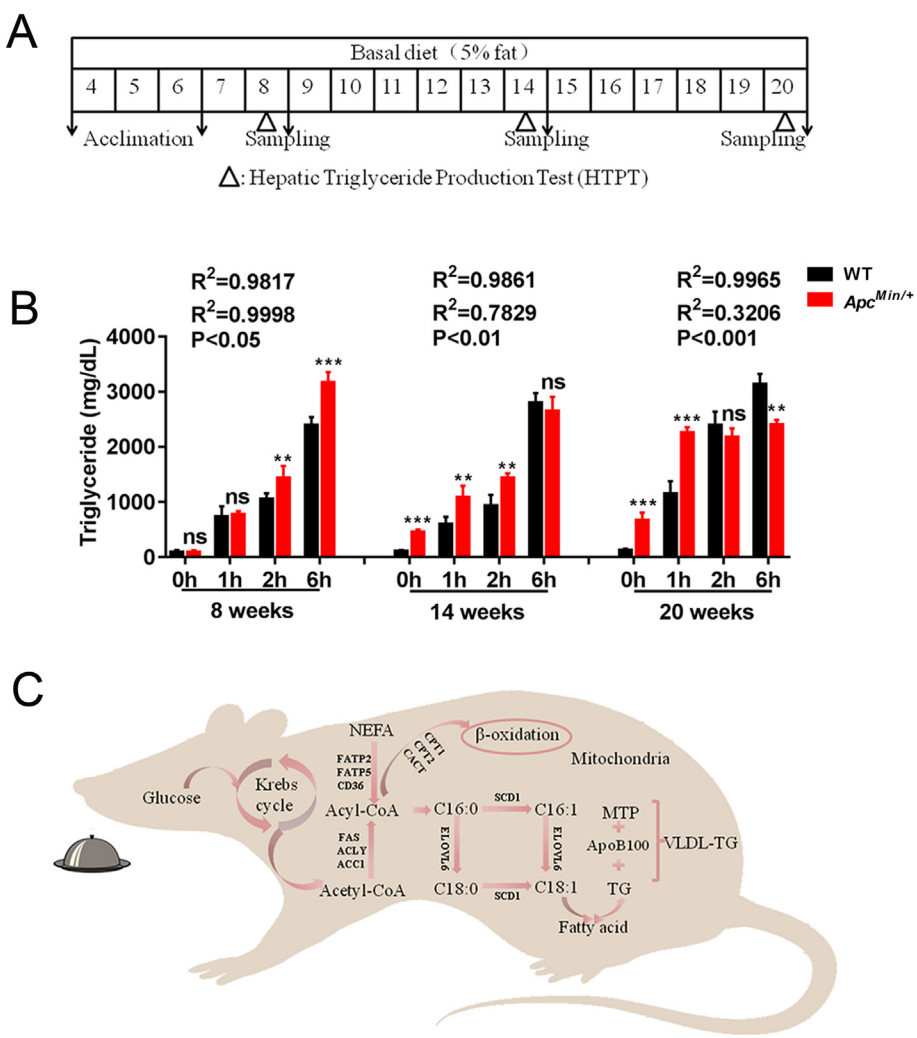

Fig. 3. Hepatic triglyceride production decreased in $Apc^{Min/+}$ mice of age. (A) A schematic of the hepatic triglyceride production test (HTPT) is shown. (B) Plasma TG levels at 0-, 1-, 2- and 6 h time points were determined via tail vein nick, and linear correlation coefficient R^2 were calculated at 0, 1 and 2 h time points in $Apc^{Min/+}$ mice and in WT mice by age ($n \geq 5$). Data are the mean of three independent experiments (an average of five readings was considered for each sample), means ± SEM. (C) Fatty acid uptake: FATP2, FATP5 and CD36 mediate transport of NEFAs across the plasma membrane. De novo lipogenesis: ACC1, ACLY and FAS are involved in the synthesis of palmitic. Palmitoyl-CoA (C16:0) was synthesized by ELOVL6 and SCD1. Fatty acid β-oxidation: acyl-CoAs are transported into mitochondria across the mitochondrial membranes by activating CPT1, CPT2 and CACAT. VLDL-TG synthesis: activated MTP, TGs are packaged together with ApoB100 to form VLDL-TG which is secreted into space of Disse [59]. FATP2/5 = fatty acid transport polypeptide 2/5; CD36 = cluster of differentiation 36; ACC1 = acetyl-CoA carboxylase 1; FAS = fatty acid synthase; ACLY = ATP Citrate Lyase; SREBP-1c = sterol regulatory element binding protein 1c; s SCD1 = stearoyl CoA desaturase 1; ELOVL6 = long-chain fatty acid elongase 6; CACT = carnitine-acyl-carnitine translocase; CPT1/2 = carnitine palmitoyltransferase 1/2; MTP = microsomal triglyceride transfer protein. Error bars represent the standard deviation. $^{**}p < 0.01$; $^{***}p < 0.001$ and ns, not significant.

age (non-cachectic), 13–14 weeks of age (pre-cachectic) and 18–20 weeks of age (severely cachectic). The mice were fasted starting at 05:00 for 4 h prior to undergoing a HTPT ($n \geq 5$). For the HTPT, the mice were intraperitoneally injected with poloxamer-407 (p-407, BASF Inc., Germany, 1000 mg/kg) from a solution (100 mg/mL) prepared by mixing the appropriate amount of room-temperature p-407 and saline under sterile conditions. Blood was collected via a tail vein nick at baseline and 1, 2, and 6 h post injection and then centrifuged at 2000 ×*g* for 10 min at 4 °C. The serum was stored at −80 °C until analysis. As previously reported, the postabsorptive TG levels normalized approximately 5–7 days post HTPT [29]. One week following HTPT, overnight-fasted mice were euthanized for tissue collection. Blood was collected via an eyeball pick at 8, 14 and 20 weeks of age. The fasting serum TG, TC and NEFA levels were determined using commercial kits from BioSino (Beijing, China).

2.3. Cell culture and treatment

HepG2 cells, obtained from Keygen Biotech (Nanjing, China, ATCC HB-8065), were maintained in Dulbecco's-modified Eagle's medium (DMEM, Gibco, USA) containing 10% FBS and antibiotics (100 unit/mL penicillin and 100 μg/mL streptomycin). The cells were incubated at 37 °C in the presence of 5% CO_2 (Thermo Scientific, CO_2 incubator). To induce an inflammatory response in the HepG2 cells, the cells were treated with media containing 10% FBS supplemented with TNFα (0, 2.5, 5, 10 ng/mL) for 24 h to investigate the regulation of Oct-1 and GPIHBP1 expression. HepG2 cells were treated with sn50 (an NF-κB inhibitor, 100 μg/mL, MedChem Express Inc., China) for 2 h and treated with TNFα (0, 5 and 10 ng/mL) for an additional 24 h to investigate which NF-κB pathways were involved in the TNFα-induced regulation of Oct-1 and GPIHBP1 expression and to investigate the total NF-κB p65 level and the phosphorylated NF-κB p65 level. All of the experiments were performed in triplicate.

2.4. Knockdown of Oct-1 and GPIHBP1 by siRNA

Oct-1 or *GPIHBP1 siRNA* and control *siRNA* were transfected into the HepG2 cells. The *siRNA* targeting the human *Oct-1* (5′-ACAGAGGUGC UAGAAAAUUAUU-3′), *GPIHBP1* (5′-AUCCUCAUCUUCCUCGUCGUA GTT-3′) and the negative control (5′-UUCUCCGAACGUGUCACG UTT-3′) were synthesized by Genepharma (Shanghai, China). The cells were cultured in six-well plates and transfected with 3 μL of 10 μM *siRNA* per well using 9 μL Lipofectamine RNAiMAX (Invitrogen, USA). After a 24 h incubation, the HepG2 cells were processed and collected for quantitative real-time PCR and Western blot analysis. Additionally, the cell-free supernatants were harvested from the culture plates by centrifugation. The TG and NEFA levels were determined using commercial kits from BioSino (Beijing, China).

2.5. H&E staining and oil red O staining

Intestinal cachexia was measured by an H&E staining Kit (Boster Inc., Beijing, China) following the manufacturer's instructions. The liver was isolated and fixed in 4% neutral-buffered formalin (Carl Roth

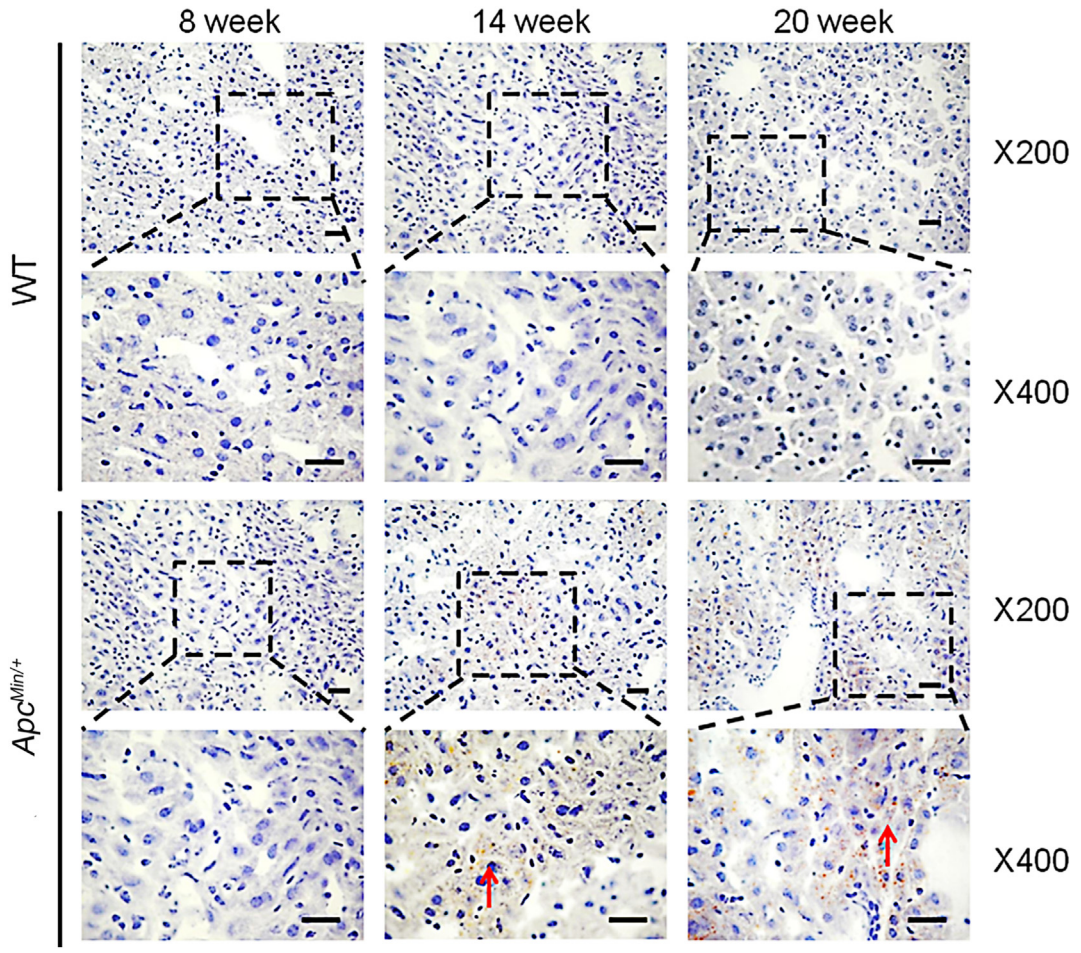

Fig. 4. Lipid droplets accumulate in the liver of $Apc^{Min/+}$ mice. Oil red O staining presented lipid droplets (red arrow) in the liver of $Apc^{Min/+}$ mouse at 14 and 20 weeks of age ($n = 3$, respectively). Magnification, ×200 and ×400. Scale bars: 50 μm. (For interpretation of the references to color in this figure legend, the reader is referred to the web version of this article.)

GmbH, Vienna, Austria). Serial sections (8 μm) of the liver were cut and stained with oil red O. Microscopic images were taken using a Nikon Eclipse E600 equipped with a Nikon Digital Sight DS-U1 unit (Spach Optics Inc., New York, USA).

2.6. Quantitative RT-PCR analysis

Total RNA from the liver of the mice was extracted by using the TRNzol (Tiangen, Beijing, China) reagent according to the manufacturer's instructions. Reverse transcription reactions were performed using the FastQuant RT kit (Tiangen, Beijing, China) to synthesize the complementary DNA (cDNA), and qRT-PCR was performed on a Bio-RadiQ5 instrument (BioRad, America) with SurperReal PreMix (Tiangen, Beijing, China) reagents using the respective gene specific-primers [30]. The primers used for gene amplification are presented in Table S1.

2.7. Western blot analysis

Protein from the liver and HepG2 cells was extracted using cell lysis buffer with inhibitors for Western blot analysis and the protein content of the supernatants was determined by using a BCA Protein Assay Kit (Beyotime, Beijing, China). Equal amounts of the protein samples were loaded into each lane of an SDS-PAGE gel followed by transfer of the protein onto a nitrocellulose membrane (Boster, Beijing, China). The membranes were incubated with primary antibodies (Table S2). Next, the membranes were incubated with a secondary antibody and imaged using a BeyoECL Plus kit (Beyotime, Beijing, China). A GAPDH and/or β-actin primary antibody (Beyotime, Beijing, China) was used as the loading control [31]. To confirm the reproducibility of the results, at least three mice per group were used in each stage or treatment of this study.

2.8. Statistical analysis

Data from the mice experiments were expressed as the means ± SEM and were analyzed using one-way ANOVA followed by Bonferroni's post hoc tests with GraphPad Prism 7.0. Data from the cells experiments were expressed as the means ± standard errors of the means (SEM) and were analyzed using one-way ANOVA followed by Tukey's post hoc tests with GraphPad Prism 7.0. $p < 0.05$ was considered statistically significant.

3. Results

The livers that were examined in our study were taken from $Apc^{Min/+}$ mice and classified as non-cachectic (8 weeks of age), pre-cachectic (14 weeks of age) and severely cachectic (20 weeks of age).

3.1. Severe hypertriglyceridemia exists in $Apc^{Min/+}$ mice

Consistently with a previous report [7], the neonatal $Apc^{Min/+}$ mice appear normal, but the $Apc^{Min/+}$ mouse displays sustained weight loss spanning approximately 5 weeks (from 16 to 20 weeks) when fed with a

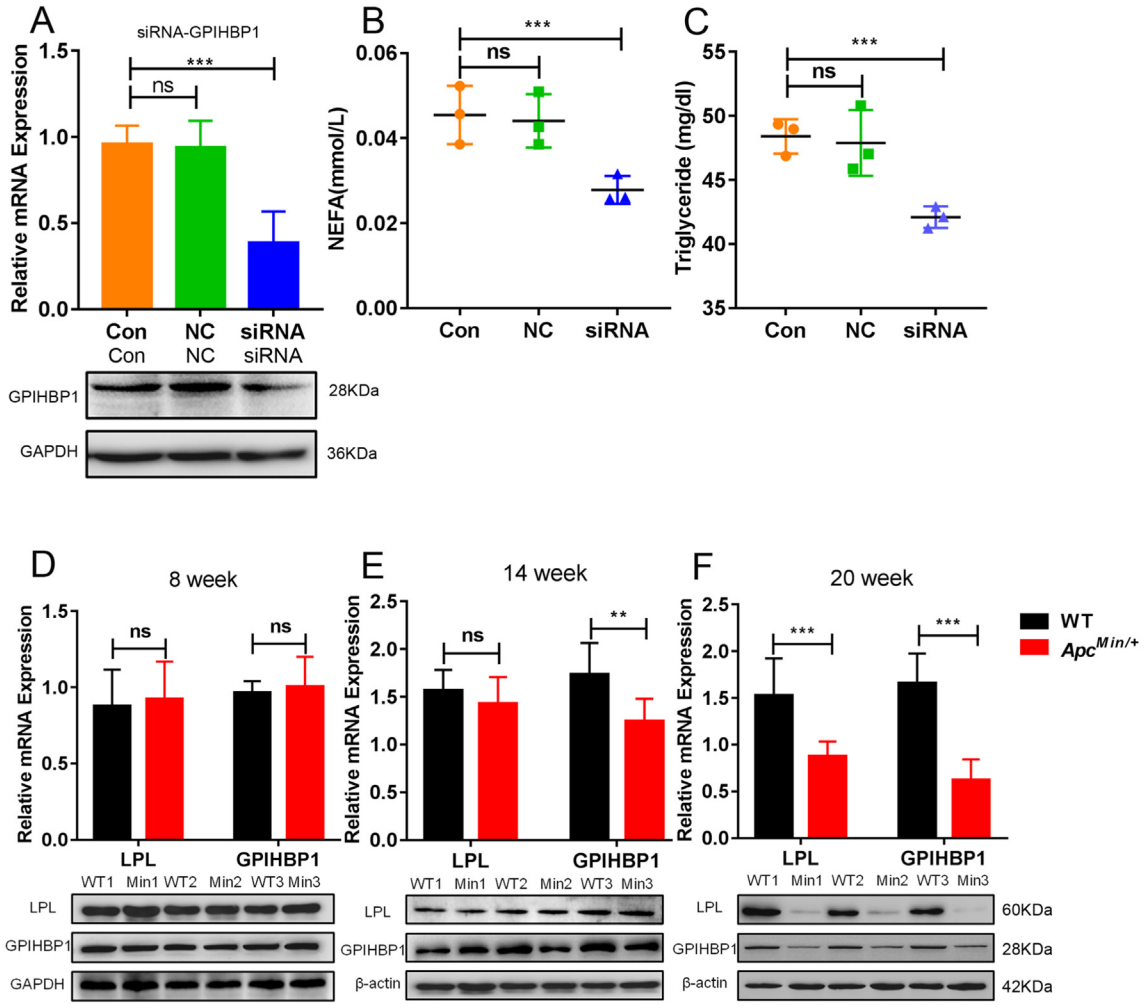

Fig. 5. GPIHBP1 plays an essential role in hypertriglyceridemia of $Apc^{Min/+}$ mice. (A–C) HepG2 cell was infected with *GPIHBP1*-specific *siRNA* or scrambled *siRNA*. GPIHBP1 expression was examined as judged by Western blot. The amount of NEFAs and TGs were measured by commercial kits (Con: indicated scrambled siRNA, NC: negative control). (D–F) LPL and GPIHBP1 expression, as judged by qRT-PCR and Western blot in the liver between the two groups at 8, 14 and 20 weeks of age ($n = 3$). All measurements were performed in triplicate. Error bars represent the standard deviation. $^{**}p < 0.01$, $^{***}p < 0.001$ and ns, not significant.

chow diet (Fig. 1A). Meanwhile, the food intake of $Apc^{Min/+}$ mice decreased by approximately 50% from 16 to 20 weeks of age (Fig. 1B). The increased triglyceride (TG) level was not present until 14 weeks of age, and severe hypertriglyceridemia was present at 20 weeks of age (Fig. 1C). A remarkable lactescence in $Apc^{Min/+}$ mice indicated that the mice had suffered from severe hyperlipidemia (Fig. 1D). Hematoxylin and eosin (H&E) staining revealed intestinal cachexia in $Apc^{Min/+}$ mice at 14 and 20 weeks of age (Fig. 1E).

3.2. Change of metabolic enzyme expression in the liver of $Apc^{Min/+}$ mice

We investigated gene expression levels of hepatic metabolic enzymes: fatty acid uptake, including fatty acid transport polypeptide (FATP2, FATP5) and cluster of differentiation 36 (CD36) [32]; De novo lipogenesis, including SREBP-1c, ACC1, ACLY, FAS, stearoyl CoA desaturase 1 (SCD1) and long-chain fatty acid elongase 6 (ELOVL6) [33]; fatty acid β-oxidation, including carnitine-acylcarnitine translocase (CACT) and carnitine palmitoyltransferase 1/2 (CPT1, CPT2) [34]. Our findings presented that hepatic *Fatp2*, *Srebp-1c*, *Acc1*, and *Acly* mRNA expression was significantly decreased in $Apc^{Min/+}$ mice, but there was no significant difference in the *CD36*, *Fatp5*, *Scd1*, *Fas*, *Elovl6*, *Cact*, *Cpt1* and *Cpt2* expression in WT mice compared to that at 20 weeks of age in $Apc^{Min/+}$ mice (Fig. 2A, B). Furthermore, western blot demonstrated that the expression of SREBP-1c, ACC1, ACLY and SCD1 was significantly decreased and there were no significant differences in the expression of FAS and ELOVL6 between the two groups at 20 weeks ($p > 0.05$, Fig. 2C). In our study, total hepatic AMPK protein and phosphorylated AMPK protein was down-regulated and phosphorylated ACC1 was up-regulated in $Apc^{Min/+}$ mice at 20 weeks ($p < 0.05$, Fig. 2D, E).

3.3. Abnormal hepatic lipid metabolism occurs during the progress of hypertriglyceridemia in $Apc^{Min/+}$ mice

In our study, at 8, 14 and 20 weeks of age, the mice were fasted for 4 h prior to undergoing a HTPT (Fig. 3A). We examined the levels of serum TGs in $Apc^{Min/+}$ and WT mice at 0-, 1-, 2- and 6-h time points at 8, 14 and 20 weeks, respectively. TG was higher in $Apc^{Min/+}$ mice than in WT mice at the 2- and 6-h time point at 8 weeks ($p < 0.01$ and $p < 0.001$, respectively), the 0-, 1- and 2-h time point at 14 weeks ($p < 0.001$, $p < 0.01$ and $p < 0.01$, respectively) and the 0- and 1-h time point at 20 weeks ($p < 0.001$ and $p < 0.001$, respectively). However, TG was lower in $Apc^{Min/+}$ mice than in wild-type (WT) mice at 6-h time point at 20 weeks ($p < 0.01$). Additionally, there was no significant difference between the WT and $Apc^{Min/+}$ mice 0- and 1-h time point at 8 weeks, the 6-h time point at 14 weeks and the 2-h time point at 20 weeks (Fig. 3B). Although TG was higher in $Apc^{Min/+}$ mice than in WT mice at some time points, the change of TG concentration

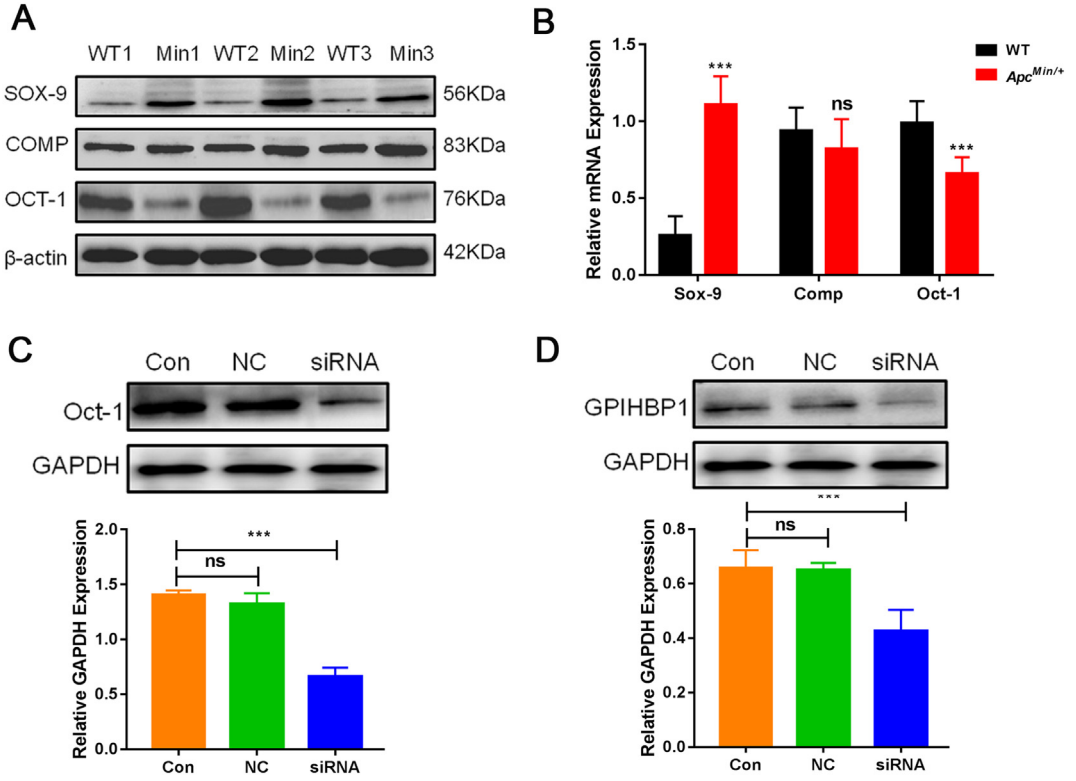

Fig. 6. Oct-1 activity regulates GPIHBP1 expression in $Apc^{Min/+}$ mice. (A, B) The expression of transcription factors in the promoter region of GPIHBP1 in mice. mRNA and protein levels, as judged by Western blot and qRT-PCR, Sox-9, Comp and Oct-1 were determined between the two groups of mice at 20 weeks of age. Data are expressed as means ± SEM. Error bars represent the standard deviation. ns, not significant, ***$p < 0.001$ versus the WT group. (C, D) HepG2 cell was infected with *Oct-1*-specific *siRNA* or scrambled *siRNA*. GPIHBP1 and Oct-1 expression were examined as judged by Western blot (Con: indicated scrambled siRNA, NC: negative control, $n = 3$). The densities of Oct-1 and GPIHBP1 bounds were measured and their ratio was calculated.

data at 0-, 1-, and 2 h time points were used to calculate hepatic TG production slopes as previously reported [29]. TG production was lower in $Apc^{Min/+}$ mice than in WT mice at 20 weeks ($Apc^{Min/+}$ group versus WT group: $R^2 = 0.3206$ versus $R^2 = 0.9965$, $p < 0.001$) and at 14 weeks ($Apc^{Min/+}$ group versus WT group: $R^2 = 0.7829$ versus $R^2 = 0.9861$, $p < 0.01$), but there was no significant difference at 8 weeks between the two groups ($Apc^{Min/+}$ group versus WT group: $R^2 = 0.9998$ versus $R^2 = 0.9817$, $p > 0.05$, Fig. 3B and Fig. S1). A schematic of hepatic fatty acid DNL, β-oxidation and fatty acid secretion in VLDL-TG in the mouse is shown in Fig. 3C. Moreover, hepatic Oil Red O staining revealed numerous fatty droplets exist in hepatocytes, indicating that centrilobular-restricted steatosis was observed in the livers of aged $Apc^{Min/+}$ mouse (Fig. 4). Therefore, we may reasonably reach the result that abnormal hepatic lipid metabolism occurs during the progress of hypertriglyceridemia in $Apc^{Min/+}$ mice.

3.4. GPIHBP1 plays an essential role in hypertriglyceridemia of $Apc^{Min/+}$ mice

To evaluate whether GPIHBP1 is involved in serum TG metabolism. We aimed to select small interference RNA (siRNA) that could efficiently inhibit GPIHBP1, which was designed specifically to the RNA genome of GPIHBP1 and introduced into HepG2 cells by lipofection transfection. 24 h post-transfection, about 50% knockdown efficacy of siRNA-GPIHBP1 for inhibiting GPIHBP1 was determined by RT-PCR and further confirmed by Western blotting (Fig. 5A). We found that siRNA- GPIHBP1 could efficiently reduce NEFA and TG production (Fig. 5B, C). Additionally, hepatic GPIHBP1 mRNA and protein levels were lower in $Apc^{Min/+}$ mice than in WT mice at 14 weeks ($p < 0.05$) and 20 weeks ($p < 0.001$). In contrast, the hepatic LPL mRNA and protein expression were lower in $Apc^{Min/+}$ mice at 20 weeks ($p < 0.001$), but there was no significant difference at 14 weeks between the two groups ($p > 0.05$) (Fig. 5D–F). Subsequently, we examined many lipid metabolism genes (APOC2, APOA5, LMF1 and APOE) that lead to hypertriglyceridemia [35–39]. There was no significant difference between the WT and $Apc^{Min/+}$ mice groups at 20 weeks (Fig. S2). Collectively, these results showed that GPIHBP1 may be one key factor contributing to hypertriglyceridemia in $Apc^{Min/+}$ mice.

3.5. TNFα regulates Oct-1 activity affecting GPIHBP1 expression via the NF-κB signaling pathway

Next, we explored the molecular mechanisms that explain why the $Apc^{Min/+}$ mice have impaired GPIHBP1 function. Our investigated the mRNA and protein expression of three transcription factors in the promoter region of GPIHBP1 including: SRY-related high mobility group-box gene 9 (Sox9) which expressed more highly in $Apc^{Min/+}$ mice than in WT mice; cartilage oligomeric matrix protein (Comp) of which the expression was not significantly different in the liver between the two groups of mice; and Oct-1 which decreased in the liver of $Apc^{Min/+}$ mice at 20 weeks (Fig. 6A, B). Previous research demonstrated that Oct-1 could be regulated by nuclear factor-κB (NF-κB)-dependent gene expression [40]. Moreover, hypertriglyceridemia dramatically inducing the increase of TRLs is associated with an inflammatory state which activates the NF-κB pathway [41]. Based on the observation, to determine whether Oct-1 is related to the regulation of GPIHBP1, We aimed to select small interference RNA (siRNA) that could efficiently inhibit Oct-1, which was designed specifically to the RNA genome of Oct-1 and introduced into HepG2 cells by lipofection transfection. 24 h post-transfection, about 60% knockdown efficacy of siRNA-Oct-1 for inhibiting Oct-1 was determined by RT-PCR and further confirmed by

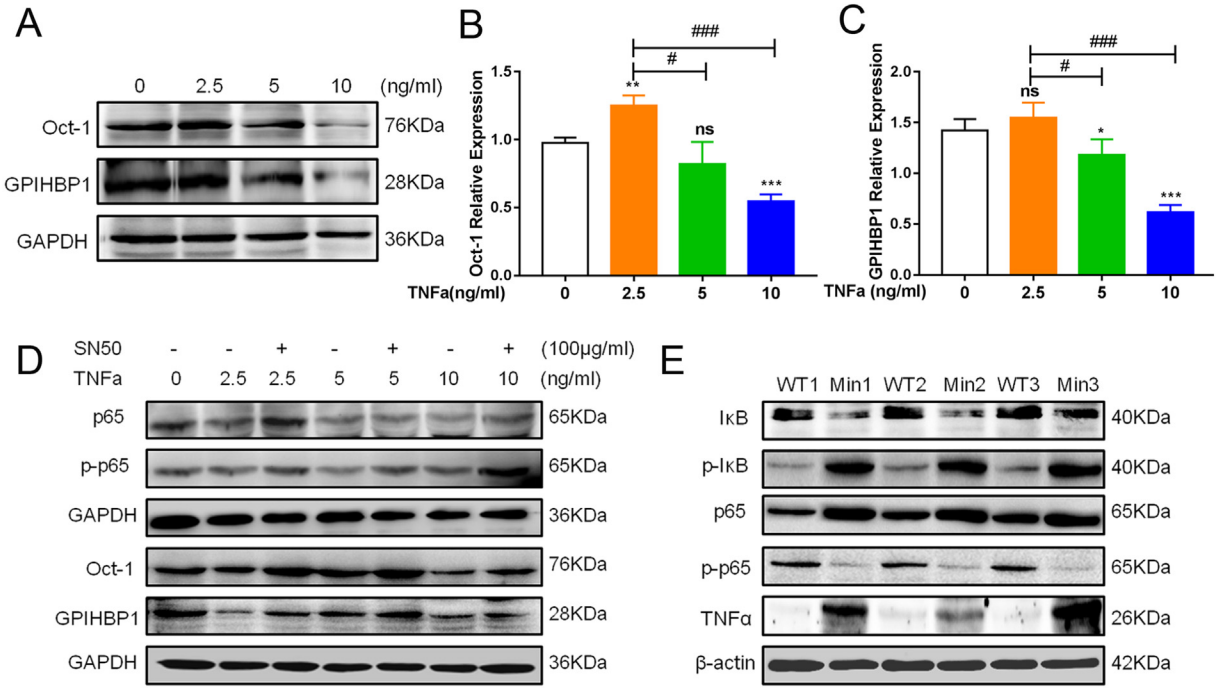

Fig. 7. TNFα regulates Oct-1 activity affecting GPIHBP1 expression via the NF-κB signaling pathway. (A–C) HepG2 cell was treated with TNFα (0, 2.5, 5, 10 ng/mL) for 24 h to determine TNFα regulates Oct-1 expression. (D) HepG2 cell was pretreated with sn50 (100 μg/mL) for 2 h and co-stimulated with TNF-α (0, 2.5, 5, 10 ng/mL) for 24 h. Whole-cell was prepared and analyzed by Western blot analysis with anti-p65 NF-κB, anti-phosphorylated NF-κB p65, anti-Oct-1 and anti-Gpihbp1 antibody. The levels of protein were normalized with GAPDH. (E) IκB, p-IκB, p65, p-p65 and TNFα protein were measured by Western blot with specific antibodies. β-actin was included as a control (WT: wild-type, Min: $Apc^{Min/+}$ mice, $n = 3$). Data are expressed as means ± SEM. Error bars represent the standard deviation. All measurements were performed in triplicate. $*p < 0.05$, $**p < 0.001$ and $***p < 0.0001$ as control group compared with treatment on TNF-α group, $\#p < 0.05$ and $\#\#\#p < 0.001$ as between-groups variance.

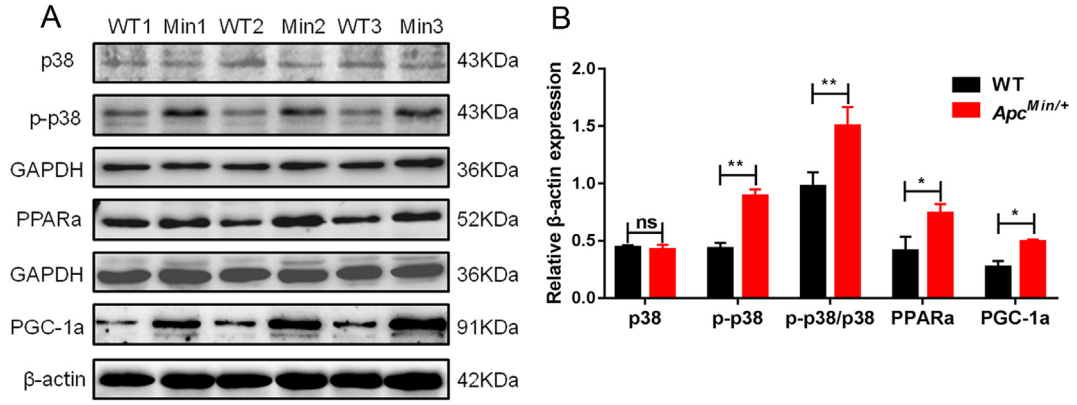

Fig. 8. p38-MAPK/PPARα pathway may be activated in the liver of $Apc^{Min/+}$ mice (A, B) Phospho-p38, p38, PGC-1α and PPARα protein were measured by Western blot with specific antibodies. β-actin and GAPDH were included as a control. (WT: wild-type, Min: $Apc^{Min/+}$ mice, $n = 3$) The densities of phosphorylated-p38, p38, PGC-1α and PPARα were measured and their ratio was calculated. Data are expressed as means ± SEM. Error bars represent the standard deviation. ns, no significant, $*p < 0.05$, and $**p < 0.01$ versus the WT group.

Western blotting (Fig. 6C, D).

Subsequently, treatment with various concentrations (0, 2.5, 5 and 10 ng/mL) of tumor necrosis factor α (TNFα) for 24 h was used to determine whether TNFα induces the NF-κB pathway and regulates Oct-1 expression in HepG2 cells. As expected, a synchronous decrease in Oct-1 and GPIHBP1 expression occurred in a dose-dependent manner of TNFα treatment (Fig. 7A–C). Furthermore, we pretreated HepG2 cells with sn50 (100 μg/mL), an inhibitor of the NF-κB pathway, for 2 h prior to TNFα stimulation for 24 h [42,43]. Here, sn50 increased TNFα-induced NF-κB p65 phosphorylation, Oct-1 and GPIHBP1 expression, with no significant differences in the total NF-κB p65 expression in the HepG2 cells (Fig. 7D). Furthermore, we used Western Blot analysis to identify that the Oct-1 is involved in the NF-κB pathway in $Apc^{Min/+}$ mice (Fig. 7E). Our results showed that the NF-κB pathway may be involved in the TNFα-regulated Oct-1 activity affecting GPIHBP1 expression in $Apc^{Min/+}$ mice and in HepG2 cells.

3.6. p38-MAPK/PPARα pathway may be activated in the liver of $Apc^{Min/+}$ mice

The p38 mitogen-activated protein kinase (p38-MAPK) is an important regulator of a broad range of genes involved in lipid metabolism [44,45]. PPARα predominantly expresses in the liver and intestinal mucosa, with high catabolic rates of fatty acids and peroxisomal metabolism [46]. Moreover, proliferator-activated receptor-γ coactivator-1α (PGC-1α) is a pivotal coactivator of PPARα and a target gene of the

p38-MAPK pathway [47,48]. Peroxisome proliferator-activated receptor-α (PPARα) and retinoid X receptors (RXRs) form a heterodimer, which binds to PPAR response elements (PPREs) in the promoter regions of target genes encoding lipid metabolic enzymes, such as LPL gene [49]. Furthermore, according to the previous report, the low expression of LPL may be associated with hyperlipidemia and involved in the progression of adenoma developing to carcinoma [3]. We used Western blot analysis to identify that the activated phosphorylated p38-MAPK activates PGC-1α and PPARα in the liver of $Apc^{Min/+}$ mice (Fig. 8A, B). Collectively, our data indicated that p38-MAPK/PPARα pathway may be activated in the liver of $Apc^{Min/+}$ mice.

4. Discussion

Cachexia is a common complication observed during end-stage cancer, and significantly affects health and vitality of life in patients. Cachexia is a metabolic syndrome characterized by severe wasting of muscle mass and adipose tissue. Thus, focusing on the complication of cachexia, i.e. the mechanisms involved in chronic inflammation and dyslipidemia is pivotal for increasing patient survial [2].

In humans, colorectal cancer is regarded as a multistep event which often involves the activation of oncogene and the loss of several tumor suppressor genes, such as APC, K-ras and p53 [50]. However, the loss of APC function has been recognized as an early event and an essential role in colorectal cancer. The $Apc^{Min/+}$ mouse is a classical model of colorectal cancer cachexia in which age-dependent hyperlipidemia state appearing in the mice is associated with the process of polyps. Development of cachexia was accompanied by the development of gut barrier dysfunction (permeability to FD4), insulin resistance and endotoxemia [9]. Interestingly, p53 and K-ras mutations, which are observed frequently in human colon cancers, are not detectable in colon tumors of $Apc^{Min/+}$ mice. Therefore, it remains unclear which event is mainly responsible for the transition from adenomas to tumors in $Apc^{Min/+}$ mice.

In the present study, we demonstrated that the $Apc^{Min/+}$ mice exhibit intestinal cachexia accompanied by associated with a loss of body weight and hypertriglyceridemia. We have found that the $Apc^{Min/+}$ mice consumed greatly less food than those of the WT group. Less food intake by $Apc^{Min/+}$ mice may partially account for their body weight loss. Moreover, several pro-inflammatory cytokines are considered as mediators of the cachectic process. TNF-α increases the corticotrophin-releasing hormone (CRH) level and decreases food intake and body weight [51]. Recent studies have confirmed that leukemia inhibitory factor (LIF) plays an essential role in lipolysis of adipocytes. LIF combining with its cognate receptor, LIFR-α, forms a coreceptor subunit gp130 which activates the JAK/STAT pathway. According to the literature, increased LIF circulating level leads to decreased adipose and body weight in mouse cancer models, which is related to cachexia [52]. Although these results strongly indicate a link between LIF and cachexia, the exact mechanism of the LIF in the cachexia to induce the loss of adipose tissue remains to be explored. Therefore, it is necessary to identify that increased LIF circulating level may account for the loss of adipose tissue in $Apc^{Min/+}$ mice.

Interestingly, in other (non-APC) colorectal cancer models, studies have shown that there are no change of serum TG in rats with colon tumors induced by 1,2-dimethylhydrazine and no increase in serum lipid levels in C57BL/6 mice with colon tumors induced by dextran sodium sulfate (DSS)/azoxymethane (AOM) [53]. Therefore, tumor development itself may not cause hyperlipidemia and it remains unclear which event is mainly responsible for the hyperlipidemia in $Apc^{Min/+}$ mice.

Since severely cachectic $Apc^{Min/+}$ mice have elevated level of serum endotoxin that is accompanied by inflammation and hyperlipidemia, which can also affect the liver [7]. To further explore and characterize hyperlipidemia, our study focused on exploring the hepatic lipid metabolism of $Apc^{Min/+}$ mice. Interestingly, as previously reported that the transcription factor *Srebp-1c* is an upstream target of phosphorylated AMPK leading to decreased *Acc1*, *Fas* and *Acly* [54]. In this study, our results suggested that the *Srebp-1c*-regulated genes (*Acc1*, *Acly*, *Fas*) in the DNL pathway were declined in the liver of $Apc^{Min/+}$ mice. Moreover, our findings presented that reduced phosphorylated AMPK and total AMPK result in the decreasing of ACC1 expression in $Apc^{Min/+}$ mice, which agrees with those reported by Fabbrini, E. and Kim, M.K. et al., who presented that the activity of the AMPK is connected with DNL in the liver [16,55,56].

Recent evidence suggests that hepatic LPL mRNA expression may be associated with hyperlipidemia and involved in the progress of intestinal polyp formation in $Apc^{Min/+}$ mice [3,4]. In our study, we further assessed the function of hepatic GPIHBP1 for the first time in $Apc^{Min/+}$ mice. Decreased GPIHBP1 expression in the capillaries may be governed by the cis-acting regulatory elements within the GPIHBP1 gene [26]. Our result indicated that NF-κB pathway regulates Oct-1 activity which affects GPIHBP1 expression in hyperlipidemia of $Apc^{Min/+}$ mice. Despite a large number of studies showing that the expression of GPIHBP1 can be a risk factor for the hyperlipidemia, the mechanisms by which GPIHBP1 induces hyperlipidemia still remain unclear in $Apc^{Min/+}$ mice.

Here, we were further interested in the mechanisms whereby GPIHBP1 induced hyperlipidemia. We used TNFα supplementation in HepG2 cell to examine the relationship between the changes of TNFα concentration and Oct-1 expression and to explore the possible underlying mechanisms. TNFα has been significantly shown to aggravate inflammatory response which is one of the pro-inflammatory cytokines. In cancer cachexia condition, TNF-α is responsible for the increase in gluconeogenesis, loss of adipose tissue, while causing a decrease in protein, glycogen and lipid synthesis [57]. In addition, some other inflammatory factors such as MCP-1 and IL-6, etc. can induce an inflammatory response and have an important effect in cachexia development of $Apc^{Min/+}$ mice [9]. Indirect evidence for the chronic inflammatory state in cachectic mice includes a number of pathological changes that are characteristic of hypertriglyceridemia and insulin resistance [58]. Therefore, to evaluate and discuss the role of the chronic inflammatory state in different metabolic alterations and muscle wasting in cancer cachexia is necessary.

Collectively, our findings suggested that TNFα as a risk factor effects Oct-1 and GPIHBP1. This elucidates a possible mechanism for the hyperlipidemia, which may explains abnormal hepatic lipid metabolism in $Apc^{Min/+}$ mice and provides insights into studying the metabolic disorders of FAP patients.

5. Conclusion

In conclusion, our study demonstrated that disordered hepatic lipid metabolism plays an essential role in hypertriglyceridemia. Additionally, the transcription factor Oct-1 influences the GPIHBP1 expression, which is involved in hypertriglyceridemia in $Apc^{Min/+}$ mice via the NF-κB pathway.

Author contributions

Conceptualization, Biao Yu, Mingjun Zhang and Xiaochun Tang; Funding acquisition, Xiaochun Tang; Investigation, Biao Yu, Jiahuan Chen, Lingyu Wang, Xinwei Zhang, Xiaohuan Peng, He Wang, Anbei Wang and Dazhong Zhao; Methodology, Biao Yu, Jiahuan Chen, Lingyu Wang, Xinwei Zhang, Xiaohuan Peng, He Wang, Anbei Wang, Dazhong Zhao and Xiaochun Tang; Project administration, Daxin Pang, Hongsheng Ouyang and Xiaochun Tang; Resources, Xiaochun Tang; Supervision, Daxin Pang, Hongsheng Ouyang and Xiaochun Tang; Writing – original draft, Biao Yu and Mingjun Zhang; Writing – review & editing, Biao Yu and Mingjun Zhang.

Conflict of interest

The authors declare no conflict of interest.

Acknowledgments

This work was financially supported by the National Natural Science Foundation of China (Grant No. 31472053 and 31572345) and Graduate Innovation Fund of Jilin University (Grant No. 2017094). The program for JLU Science and Technology Innovative Research Team (JLUSTIRT, No. 2017TD-28), the Fundamental Research Funds for the Central Universities.

Appendix A. Supplementary data

Supplementary data to this article can be found online at https://doi.org/10.1016/j.lfs.2019.04.041.

References

[1] J. Inagaki, V. Rodriguez, G.P. Bodey, Proceedings: causes of death in cancer patients, Cancer 33 (1974) 568–573.
[2] J. Bachmann, H. Friess, M.E. Martignoni, Molecular mechanisms and its clinical impact in cancer cachexia, Zeitschrift fur Gastroenterologie 46 (2008) 1384–1392.
[3] Naoko Niho, Mami Takahashi, Tomohiro Kitamura, Yutaka Shoji, Masaki Itoh, Tetsuo Noda, Takashi Sugimura, K. Wakabayashi, Concomitant suppression of hyperlipidemia and intestinal polyp formation in Apc-deficient mice by peroxisome proliferator-activated receptor ligands, Cancer Res. 63 (2003) 6090–6095.
[4] Naoko Niho, Mami Takahashi, Yutaka Shoji, Yoshito Takeuchi, Satoshi Matsubara, Takashi Sugimura Keiji, K. Wakabayashi, Dose-dependent suppression of hyperlipidemia and intestinal polyp formation in Min mice by pioglitazone, a PPARγ ligand, Cancer Sci. 94 (2003) 960–964.
[5] Y. Li, S.X. Cui, S.Y. Sun, W.N. Shi, Z.Y. Song, S.Q. Wang, X.F. Yu, Z.H. Gao, X.J. Qu, Chemoprevention of intestinal tumorigenesis by the natural dietary flavonoid myricetin in APCMin/+ mice, Oncotarget 7 (2016) 60446–60460.
[6] Silvia Speca, Laurent Dubuquoy, Pierre Desreumaux, Peroxisome proliferator–activated receptor gamma in the colon inflammation and innate antimicrobial immunity, J. Clin. Gastroenterol. 48 (2014) 23–27.
[7] A.A. Narsale, R.T. Enos, M.J. Puppa, S. Chatterjee, E.A. Murphy, R. Fayad, M.O. Pena, J.L. Durstine, J.A. Carson, Liver inflammation and metabolic signaling in ApcMin/+ mice: the role of cachexia progression, PLoS One 10 (2015) e0119888.
[8] Z. Liu, Y. Xiao, Z. Zhou, X. Mao, J. Cai, L. Xiong, C. Liao, F. Huang, Z. Liu, M.S. Ali Sheikh, J. Plutzky, H. Huang, T. Yang, Q. Duan, Extensive metabolic disorders are present in APC(min) tumorigenesis mice, Mol. Cell. Endocrinol. 427 (2016) 57–64.
[9] M.J. Puppa, J.P. White, S. Sato, M. Cairns, J.W. Baynes, J.A. Carson, Gut barrier dysfunction in the ApcMin/+ mouse model of colon cancer cachexia, Bba-Mol Basis Dis 1812 (2011) 1601–1606.
[10] K.A. Baltgalvis, F.G. Berger, M.M.O. Pena, J.M. Davis, S.J. Muga, J.A. Carson, Interleukin-6 and cachexia in Apc(Min/+) mice, Am J Physiol-Reg I 294 (2008) R393–R401.
[11] M. Mutoh, T. Akasu, M. Takahashi, N. Niho, T. Yoshida, T. Sugimura, K. Wakabayashi, Possible involvement of hyperlipidemia in increasing risk of colorectal tumor development in human familial adenomatous polyposis, Jpn. J. Clin. Oncol. 36 (2006) 166–171.
[12] W.R. Bruce, T.M. Wolever, A. Giacca, Mechanisms linking diet and colorectal cancer: the possible role of insulin resistance, Nutr. Cancer 37 (2000) 19–26.
[13] R. Jarvinen, P. Knekt, T. Hakulinen, H. Rissanen, M. Heliovaara, Dietary fat, cholesterol and colorectal cancer in a prospective study, Br. J. Cancer 85 (2001) 357–361.
[14] O. Ates, B. Sivri, S. Kilickap, Evaluation of risk factors for the recurrence of colorectal polyps and colorectal cancer, Turkish journal of medical sciences 47 (2017) 1370–1376.
[15] N. Harada, Z. Oda, Y. Hara, K. Fujinami, M. Okawa, K. Ohbuchi, M. Yonemoto, Y. Ikeda, K. Ohwaki, K. Aragane, Y. Tamai, J. Kusunoki, Hepatic de novo lipogenesis is present in liver-specific ACC1-deficient mice, Mol. Cell. Biol. 27 (2007) 1881–1888.
[16] E. Fabbrini, F. Magkos, Hepatic steatosis as a marker of metabolic dysfunction, Nutrients 7 (2015) 4995–5019.
[17] M.C. Lee, J. Han, S.H. Lee, D.H. Kim, H.M. Kang, E.J. Won, D.S. Hwang, J.C. Park, A.S. Om, J.S. Lee, A brominated flame retardant 2,2′,4,4′ tetrabrominated diphenyl ether (BDE-47) leads to lipogenesis in the copepod Tigriopus japonicus, Aquat. Toxicol. 178 (2016) 19–26.
[18] J. Sanchez-Gurmaches, Y. Tang, N.Z. Jespersen, M. Wallace, C. Martinez Calejman, S. Gujja, H. Li, Y.J.K. Edwards, C. Wolfrum, C.M. Metallo, S. Nielsen, C. Scheele, D.A. Guertin, Brown fat AKT2 is a cold-induced kinase that stimulates ChREBP-mediated de novo lipogenesis to optimize fuel storage and thermogenesis, Cell Metab. 27 (2018) 195–209 (e196).
[19] A.P. Jensen-Urstad, C.F. Semenkovich, Fatty acid synthase and liver triglyceride metabolism: housekeeper or messenger? Biochim. Biophys. Acta 1821 (2012) 747–753.
[20] J.A. Duarte, F. Carvalho, M. Pearson, J.D. Horton, J.D. Browning, J.G. Jones, S.C. Burgess, A high-fat diet suppresses de novo lipogenesis and desaturation but not elongation and triglyceride synthesis in mice, J. Lipid Res. 55 (2014) 2541–2553.
[21] J. Dai, K. Liang, S. Zhao, W. Jia, Y. Liu, H. Wu, J. Lv, C. Cao, T. Chen, S. Zhuang, X. Hou, S. Zhou, X. Zhang, X.W. Chen, Y. Huang, R.P. Xiao, Y.L. Wang, T. Luo, J. Xiao, C. Wang, Chemoproteomics reveals baicalin activates hepatic CPT1 to ameliorate diet-induced obesity and hepatic steatosis, Proc. Natl. Acad. Sci. U. S. A. 115 (2018) E5896–E5905.
[22] G. Haemmerle, R. Zimmermann, J.G. Strauss, D. Kratky, M. Riederer, G. Knipping, R. Zechner, Hormone-sensitive lipase deficiency in mice changes the plasma lipid profile by affecting the tissue-specific expression pattern of lipoprotein lipase in adipose tissue and muscle, J. Biol. Chem. 277 (2002) 12946–12952.
[23] H. Adachi, T. Kondo, G.Y. Koh, A. Nagy, Y. Oike, E. Araki, Angptl4 deficiency decreases serum triglyceride levels in low-density lipoprotein receptor knockout mice and streptozotocin-induced diabetic mice, Biochem. Biophys. Res. Commun. 409 (2011) 177–180.
[24] B.S. Davies, A.P. Beigneux, R.H. Barnes 2nd, Y. Tu, P. Gin, M.M. Weinstein, C. Nobumori, R. Nyren, I. Goldberg, G. Olivecrona, A. Bensadoun, S.G. Young, L.G. Fong, GPIHBP1 is responsible for the entry of lipoprotein lipase into capillaries, Cell Metab. 12 (2010) 42–52.
[25] L.G. Fong, S.G. Young, A.P. Beigneux, A. Bensadoun, M. Oberer, H. Jiang, M. Ploug, GPIHBP1 and plasma triglyceride metabolism, Trends Endocrinol Metab 27 (2016) 455–469.
[26] O. Adeyo, C.N. Goulbourne, A. Bensadoun, A.P. Beigneux, L.G. Fong, S.G. Young, Glycosylphosphatidylinositol-anchored high-density lipoprotein-binding protein 1 and the intravascular processing of triglyceride-rich lipoproteins, J. Intern. Med. 272 (2012) 528–540.
[27] M.M. Weinstein, L. Yin, Y. Tu, X. Wang, X. Wu, L.W. Castellani, R.L. Walzem, A.J. Lusis, L.G. Fong, A.P. Beigneux, S.G. Young, Chylomicronemia elicits atherosclerosis in mice–brief report, Arterioscler. Thromb. Vasc. Biol. 30 (2010) 20–23.
[28] M.M. Veniant, A.P. Beigneux, A. Bensadoun, L.G. Fong, S.G. Young, Lipoprotein size and susceptibility to atherosclerosis - insights from genetically modified mouse models, Curr. Drug Targets 9 (2008) 174–189.
[29] K.D. Ono-Moore, M. Ferguson, M.L. Blackburn, H. Issafras, S.H. Adams, Application of an in vivo hepatic triacylglycerol production method in the setting of a high-fat diet in mice, Nutrients 9 (2016).
[30] M. Li, H. Ouyang, H. Yuan, J. Li, Z. Xie, K. Wang, T. Yu, M. Liu, X. Chen, X. Tang, H. Jiao, D. Pang, Site-specific Fat-1 knock-in enables significant decrease of n-6PUFAs/n-3PUFAs ratio in pigs, G3 8 (2018) 1747–1754.
[31] S. Sun, M. Zhang, Q. Yang, Z. Shen, J. Chen, B. Yu, H. Wang, J. Qu, D. Pang, W. Ren, H. Ouyang, X. Tang, Resveratrol suppresses lipoprotein-associated phospholipase A2 expression by reducing oxidative stress in macrophages and animal models, Mol. Nutr. Food Res. 61 (2017).
[32] J.F. Ge, J.L. Walewski, D. Anglade, P.D. Berk, Regulation of hepatocellular fatty acid uptake in mouse models of fatty liver disease with and without functional leptin signaling: roles of NfKB and SREBP-1C and the effects of Spexin, Semin. Liver Dis. 36 (2016) 360–372.
[33] R. Khound, J. Taher, C. Baker, K. Adeli, Q.Z. Su, GLP-1 elicits an intrinsic gut-liver metabolic signal to ameliorate diet-induced VLDL overproduction and insulin resistance, Arterioscl Throm Vas 37 (2017) 2252.
[34] L. Koletzko, A. Mahli, C. Hellerbrand, Development of an in vitro model to study hepatitis C virus effects on hepatocellular lipotoxicity and lipid metabolism, Pathol. Res. Pract. 214 (2018) 1700–1706.
[35] S. Kersten, Triglyceride metabolism under attack, Cell Metab. 25 (2017) 1209–1210.
[36] J.J. Jiang, Y.H. Wang, Y. Ling, A. Kayoumu, G. Liu, X. Gao, A novel APOC2 gene mutation identified in a Chinese patient with severe hypertriglyceridemia and recurrent pancreatitis (vol 15, pg 12, 2016), Lipids Health Dis. 15 (2016).
[37] W. Khovidhunkit, S. Charoen, A. Kiateprungvej, P. Chartyingcharoen, S. Muanpetch, W. Plengpanich, Rare and common variants in LPL and APOA5 in Thai subjects with severe hypertriglyceridemia: a resequencing approach, Journal of clinical lipidology 10 (2016) 505–511 (e501).
[38] A.B. Cefalu, R. Spina, D. Noto, V. Ingrassia, V. Valenti, A. Giammanco, F. Fayer, G. Misiano, G. Cocorullo, C. Scrimali, O. Palesano, G.I. Altieri, A. Ganci, C.M. Barbagallo, M.R. Averna, Identification of a novel LMF1 nonsense mutation responsible for severe hypertriglyceridemia by targeted next-generation sequencing, Journal of clinical lipidology 11 (2017) 272–281 (e278).
[39] F.M. Sacks, The crucial roles of apolipoproteins E and C-III in apoB lipoprotein metabolism in normolipidemia and hypertriglyceridemia, Curr. Opin. Lipidol. 26 (2015) 56–63.
[40] N.G. dela Paz, S. Simeonidis, C. Leo, D.W. Rose, T. Collins, Regulation of NF-kappaB-dependent gene expression by the POU domain transcription factor Oct-1, J. Biol. Chem. 282 (2007) 8424–8434.
[41] G.D. Norata, L. Grigore, S. Raselli, L. Redaelli, A. Hamsten, F. Maggi, P. Eriksson, A.L. Catapano, Post-prandial endothelial dysfunction in hypertriglyceridemic subjects: molecular mechanisms and gene expression studies, Atherosclerosis 193 (2007) 321–327.
[42] Q.B. Yang, H.M. Yuan, M. Chen, J.L. Qu, H. Wang, B.A. Yu, J.H. Chen, S.N. Sun, X.C. Tang, W.Z. Ren, Metformin ameliorates the progression of atherosclerosis via suppressing macrophage infiltration and inflammatory responses in rabbits, Life Sci. 198 (2018) 56–64.
[43] Y.X. Sun, D.K. Dai, R. Liu, T. Wang, C.L. Luo, H.J. Bao, R. Yang, X.Y. Feng, Z.H. Qin, X.P. Chen, L.Y. Tao, Therapeutic effect of SN50, an inhibitor of nuclear factor-kappaB, in treatment of TBI in mice, Neurological sciences: official journal of the

Italian Neurological Society and of the Italian Society of Clinical Neurophysiology 34 (2013) 345–355.
[44] G. Ashabi, M. Ramin, P. Azizi, Z. Taslimi, S.Z. Alamdary, A. Haghparast, N. Ansari, F. Motamedi, F. Khodagholi, ERK and p38 inhibitors attenuate memory deficits and increase CREB phosphorylation and PGC-1alpha levels in Abeta-injected rats, Behav. Brain Res. 232 (2012) 165–173.
[45] C. Fu, L. Liu, F. Li, Acetate alters the process of lipid metabolism in rabbits, Animal 12 (2018) 1895–1902.
[46] K. Schoonjans, B. Staels, J. Auwerx, The peroxisome proliferator activated receptors (PPARS) and their effects on lipid metabolism and adipocyte differentiation, Biochim. Biophys. Acta 1302 (1996) 93–109.
[47] I. Irrcher, D.A. Hood, Regulation of Egr-1, SRF, and Sp1 mRNA expression in contracting skeletal muscle cells, J. Appl. Physiol. 97 (2004) 2207–2213.
[48] E. Jirkovsky, O. Popelova, P. Krivakova-Stankova, A. Vavrova, M. Hroch, P. Haskova, E. Brcakova-Dolezelova, S. Micuda, M. Adamcova, T. Simunek, Z. Cervinkova, V. Gersl, M. Sterba, Chronic anthracycline cardiotoxicity: molecular and functional analysis with focus on nuclear factor erythroid 2-related factor 2 and mitochondrial biogenesis pathways, J. Pharmacol. Exp. Ther. 343 (2012) 468–478.
[49] K. Schoonjans, J. Peinado-Onsurbe, A.M. Lefebvre, R.A. Heyman, M. Briggs, S. Deeb, B. Staels, J. Auwerx, PPARalpha and PPARgamma activators direct a distinct tissue-specific transcriptional response via a PPRE in the lipoprotein lipase gene, EMBO J. 15 (1996) 5336–5348.
[50] Y. Yamada, H. Mori, Multistep carcinogenesis of the colon in Apc(Min/+) mouse, Cancer Sci. 98 (2007) 6–10.
[51] N. Vaisman, T. Hahn, Tumor necrosis factor-alpha and anorexia–cause or effect? Metab. Clin. Exp. 40 (1991) 720–723.
[52] G.K. Arora, A. Gupta, S. Narayanan, T. Guo, P. Iyengar, R.E. Infante, Cachexia-associated adipose loss induced by tumor-secreted leukemia inhibitory factor is counterbalanced by decreased leptin, JCI insight 3 (2018).
[53] T.P. Barton, J.P. Cruse, M.R. Lewin, Changes in serum lipids related to the presence of experimental colon cancer, Br. J. Cancer 56 (1987) 451–454.
[54] M. You, M. Matsumoto, C.M. Pacold, W.K. Cho, D.W. Crabb, The role of AMP-activated protein kinase in the action of ethanol in the liver, Gastroenterology 127 (2004) 1798–1808.
[55] M.K. Kim, S.H. Kim, H.S. Yu, H.G. Park, U.G. Kang, Y.M. Ahn, Y.S. Kim, The effect of clozapine on the AMPK-ACC-CPT1 pathway in the rat frontal cortex, Int. J. Neuropsychopharmacol. 15 (2012) 907–917.
[56] H.M. O'Neill, G.P. Holloway, G.R. Steinberg, AMPK regulation of fatty acid metabolism and mitochondrial biogenesis: implications for obesity, Mol. Cell. Endocrinol. 366 (2013) 135–151.
[57] H.J. Patel, B.M. Patel, TNF-alpha and cancer cachexia: molecular insights and clinical implications, Life Sci. 170 (2017) 56–63.
[58] J. Siebler, P.R. Galle, M.M. Weber, The gut-liver-axis: endotoxemia, inflammation, insulin resistance and NASH, J. Hepatol. 48 (2008) 1032–1034.
[59] Y. Kawano, D.E. Cohen, Mechanisms of hepatic triglyceride accumulation in non-alcoholic fatty liver disease, J. Gastroenterol. 48 (2013) 434–441.